**July 5, 2023**

**FP44: Zeeman Spectroscopy**

Brandt M., Provencio Lameiras, J.C. Tutor: Ackerman, N.

## Contents

# 1. Introduction

# 2. Part I: Spectroscopy of the Zeeman Effect

## 2.1 Magnetic field strength and hystersis effect

We can observe in Figure 1, that the effect of hysteresis in the magnetic field is negligible for increasing and decreasing current. A good measure of it would be the deviation of parameters in the two linear fits. Especially we will consider in the discussion the intersection with the y-axis, or the parameter $b$ of a linear fit

$$f(x) = ax + b. \tag{1}$$

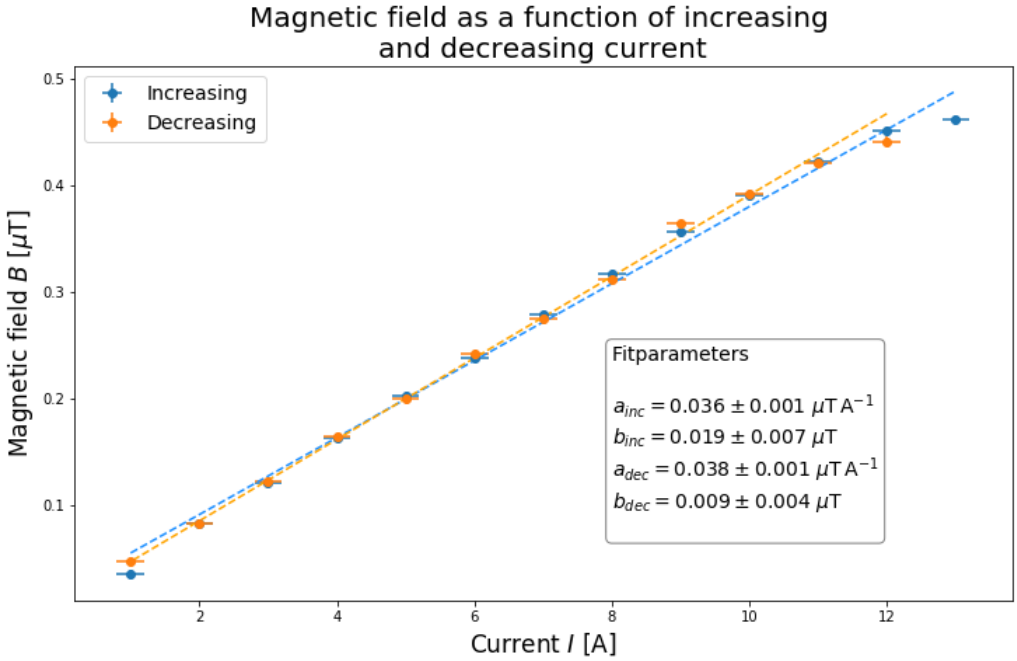


**Figure 1:** Magnetic field strength with increasing and decreasing current

The following measures we will take at the currents $I = \{8, 9, 11, 12\}$ A so we will highlight in Table 1 the magnetic fields at these positions as determined by the linear fits in Figure 1. We take the mean of the results and the standard deviation.

| $I$ [A] | 8 | 9 | 11 | 12 |
|---|---|---|---|---|
| $B$ [$\mu$T] | 0.311(3) | 0.348(4) | 0.422(6) | 0.459(7) |

**Table 1:** Relevant magnetic field strengths

## 2.2 Positions of all the Peaks in the Zeeman spectra

In total four measurements were taken at varyiing currents $I = \{8, 9, 11, 12\}\,\mathrm{A}$. For demonstrative purposes, we will conduct this part of the evaluation using the measurement for $I = 12\,\mathrm{A}$ and include the rest of the relevant plots and information in the annex (Table 4.2).

Once we have a clean image of the spectrum, we can begin by determining the positions of all the peaks and continue by fitting a triple gaussian around them. We generally use a gaussian function, because it best describes the intensity distribution of a light spectrum around a spectral line. The position of all the maxima were found with a peak finding algorithm and subsequently we fitted the gaussian distribution automatically over the estimated parameters. For that we had to first clean up our data, meaning removing the last order, from which only two of the three peaks are visible. For the fit we also concentrated on the region around each order, without taking into account the entire distribution, which makes the determination of the parameters quite difficult. The results are graphed in Figure 2.

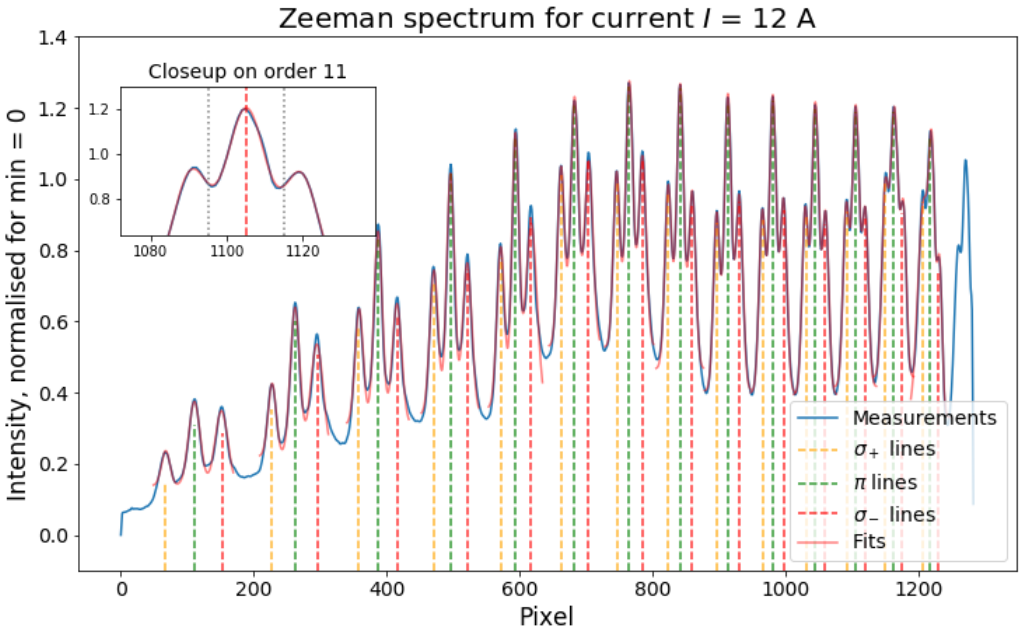


**Figure 2:** Slice of spectral distribution, fitted with triple gaussians around each order. The $\pi$-line is respectively highlighted with a red dashed line and the $\sigma$-lines surrounding it with yellow dashed lines. Within the closeup of order 11 is the certainty interval of $1\sigma$ given by the dotted gray lines around the $\pi$-line with a dashed red line

In the closeup to the 11th order we can see a quite satisfactory overlap between our measurements and the fit we found. This is simlar for all of the orders. What the fit in general often fails to achieve is the offset $d$, towards which the gaussian functions approach

asymptotically. This means in general, that the amplitude of the peaks is also off by that amount. This is for the moment not important to us because we're not interested in the amplitude, but in the position of the peaks.

The "exact" position are given by the gaussian fit

$$f(x) = a \exp\left\{-\frac{(x-b)^2}{2c^2}\right\} + d \qquad (2)$$

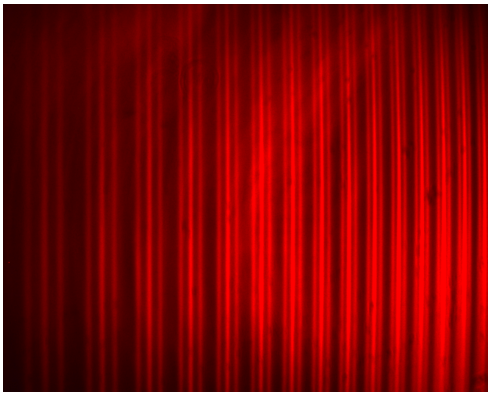

**Figure 3:** Camera image of Zeemann spectrum

and the error estimated is the square root of the covariance. This error is in the order smaller than a single pixel, so we can conclude that it is massively underestimated. What we can do instead is take a look at the $1\sigma$-Interval of a gaussian Integral, where roughly 65% of the area is concentrated. For (2), integrating from $[-c, c]$ gives us the $1\sigma$-interval. We could also use the $2\sigma$-interval if we wanted a 95% certainty, but this is in our case not necessary, since the peaks are mostly well defined and pretty sharp. We thus give the error of our position with the parameter $c$. In **??** we can see the error-interval marked by two dotted gray lines. For the peaks of smaller order this works very well, however the higher order peaks have bigger errors and thus the $1\sigma$-intervals of the $\pi$ and $\sigma$-lines overlap significantly. We can also see this effect in **??** in the next section, where we plot the order of the peak against its position.

### 2.3 Interference order against line position

In the following, we plot the orders of intereference against its positions and immediately fit a polynomial function over it. We find that a polynome of second order is sufficient to describe their relation

$$k(x) = ax^2 + bx + c, \qquad (3)$$

$$\Delta k(x) = \sqrt{(\Delta a\, x^2)^2 + (2a\Delta x)^2 + (\Delta b\, x)^2 + (b\Delta x)^2 + (\Delta c)^2}. \qquad (4)$$

We determine the optimal parameters for the second order polynomial using the measurements from the $\pi$-line and subsequently use these parameters to plot the measurements for the $\sigma$-lines over this line. We use the fit, pictured in Figure 4.

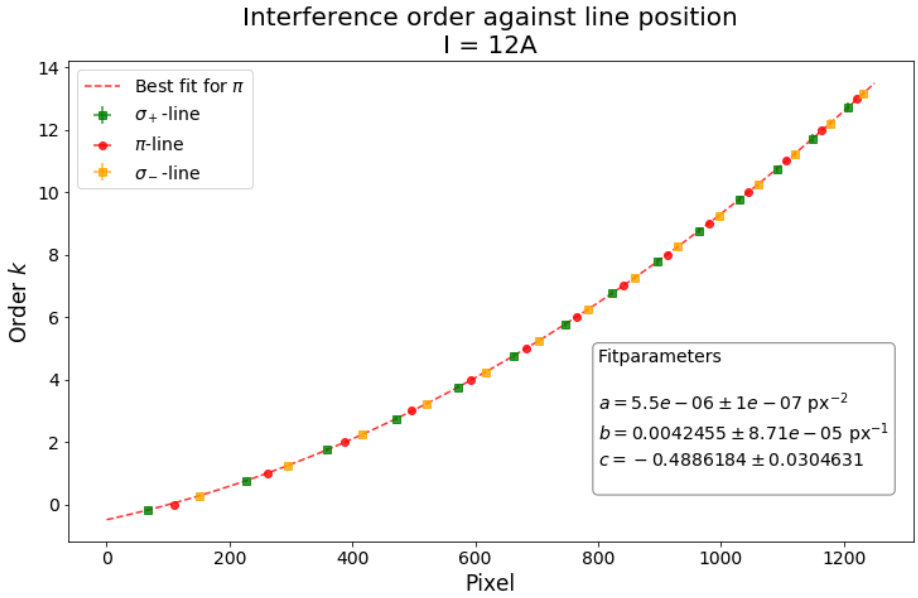


**Figure 4:** Plot of the interference order $k$ against position of peaks. A fit was determined using a polynomial of second order (3) and the order of the lateral $\sigma$-lines was plotted on top of the fit given the determined positions from subsection 2.2

The error of the lateral $\sigma$-lines in the $x$-direction was given with the $1\sigma$-deviation like for the $\pi$-line. In $y$-direction we used gaussian error propagation for (3). Based on the distances between the lines we have previously determined with the gaussian fits, we determine the relation

$$\frac{\delta a}{\Delta a} = 0.291(4) \tag{5}$$

with $\delta a$ being the distance between two peaks within the same order and $\Delta a$ the distance between the peaks of two neighbouring orders. We find by plotting them against each other a linear relationship and and determine the value $\frac{\delta a}{\Delta a}$ using a corresponding linear fit. We can see the relation up close in Figure 5. We also find a proportionality trend in which this relation rises with rising current. The results can be found in the annex and in Table 2.

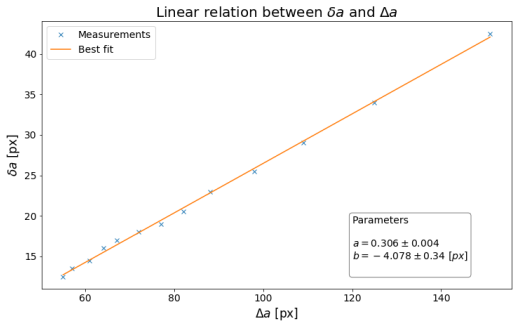


**Figure 5:** Relation between $\delta a$ and $\Delta a$. Interpolation of a linear fit to determine parameter $\frac{\delta a}{\Delta a}$

| $I$ [A] | 8 | 9 | 11 | 12 |
|---|---|---|---|---|
| $\frac{\delta a}{\Delta a}$ | 0.213(4) | 0.246(5) | 0.291(4) | 0.306(5) |

**Table 2:** $\frac{\delta a}{\Delta a}$ for varyiing current measurements

We can consequently use this value to determine the shift in wavelength $\delta\lambda$ per

$$\delta\lambda = \frac{\delta a}{\Delta a} \cdot \frac{\lambda^2}{2d\sqrt{n^2-1}} \tag{6}$$

Where $\lambda$ will be the wavelength of the cadmium lamp, which we will determine in subsection 3.2, $d = 4,04\,\text{mm}$ is the thickness of the Lummer-Gehrcke Plate and $n = 1,4567$ is its refraction index. With a wavelength of

$$\lambda_{\text{Cd}} = 643.88(23)\,\text{nm} \tag{7}$$

we can complete Table 2 with the corresponding wavelength shifts $\delta\lambda$ in Table 3

| $I$ [A] | 8 | 9 | 11 | 12 |
|---|---|---|---|---|
| $\frac{\delta a}{\Delta a}$ | 0.213(4) | 0.246(5) | 0.291(4) | 0.306(5) |
| $\delta\lambda$ nm | 0.01031(19) | 0.01189(22) | 0.01408(20) | 0.01480(18) |

**Table 3:** $\delta\lambda$ for varyiing current measurements

### 2.4 Bohr Magneton

With this information we can now determine the Bohr Magneton per (10) [1]

$$\mu_{\text{B}} = \frac{\Delta E_{\text{pot}}}{m_l \cdot B}. \tag{8}$$

whereas

$$E_{\text{pot}} = \frac{hc}{\lambda} \qquad\qquad \Delta E_{\text{pot}} = hc\left(\frac{1}{\lambda} - \frac{1}{\lambda + \delta\lambda}\right) \tag{9}$$

We consider Cadmium with an electronic configuration where the total spin is $S = 0$. In this case, (8) reduces to

$$\mu_{\text{B}} = \frac{\Delta E_{\text{pot}}}{M_J B} \tag{10}$$

$$\Delta\mu_{\text{B}} = \mu_{\text{B}}\sqrt{\left(\frac{\Delta(\Delta E_{\text{pot}})}{(\Delta E_{\text{pot}})}\right)^2 + \left(\frac{\Delta B}{B}\right)^2} \tag{11}$$

where we observe the transitions for $M_J = 1$ (?). The magnetic field was determined in subsection 2.1. The values for the Bohr Magneton in every measurement are depicted in Table 4.

| $I$ [A] | 8 | 9 | 11 | 12 | Mean |
|---|---|---|---|---|---|
| $\mu_B$ $[10^{-24}\,JT^{-1}]$ | 15.89(17) | 16.38(20) | 15.99(24) | 15.45(25) | 15.9(3) |

**Table 4:** Calculation of the Bohr Magneton for every measurement

# 3. Precision spectroscopy

## 3.1 Calibration

From the precision measurement we fit the 4 neon lines to calibrate between our unit of measurements from pixels to wavelengths. The spectrum can be appreciated in Figure 6. In the camera image, we can see that only 3 of the 4 lines we were looking for can be resolved with the apparatus. There is room for interpretation for the 4th one being on the far right end of the image, but it is too dim to separate it from the third one. Based on the relative distances between the spectral lines and their relative intensity to each other, we make an educated assumption and attribute the furthermost left line to the wavelength $\lambda_1 = 650.653$, the middle and brightest line $\lambda_2 = 640.225$ and the furthermost right line $\lambda = 638.299$. The reason why they're in reverse order is likely the position of the camera. In Figure 7 we can see a slice of the intensities and within the diagram also the linear fit that was used for calibration.

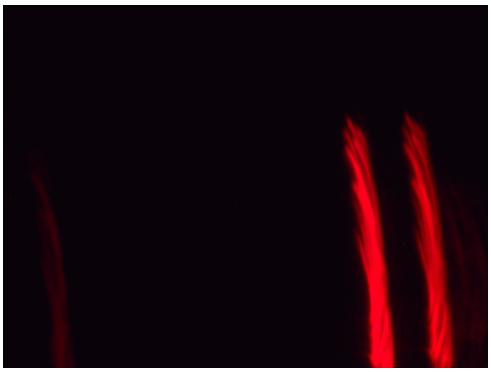

**Figure 6:** Camera image of the neon spectrum, taken at the wavelength interval of the Czerny-Turner monochromator of [621-632]

## 3.2 Cadmium line

In the following we determine the wavelength of the cadmium line. This we can do by observing the combined neon and cadmium spectrum and determining the position of the cadmium line relative to the neon spectrum. For this we converted the pixel unit to a wavelength using the linear fit from Figure 7. The wavelength of the Cadmium line was determined similarly by fitting a single gaussian curve and using the $1\sigma$-interval as an appropriate error. Reiterating what we see in Figure 8, we get a value of

$$\lambda_{Cd} = 643.88(23)\,\text{nm} \tag{12}$$

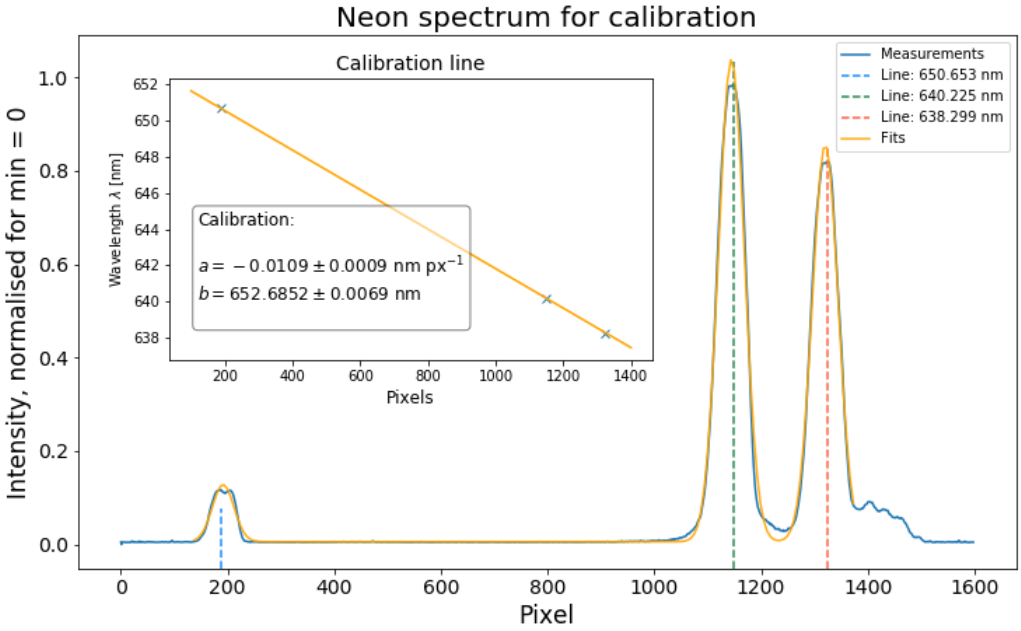


**Figure 7:** Diagram of the intensities of the 3 resolved neon lines with a linear fit for the pixel to wavelength conversion based on the previous estimations

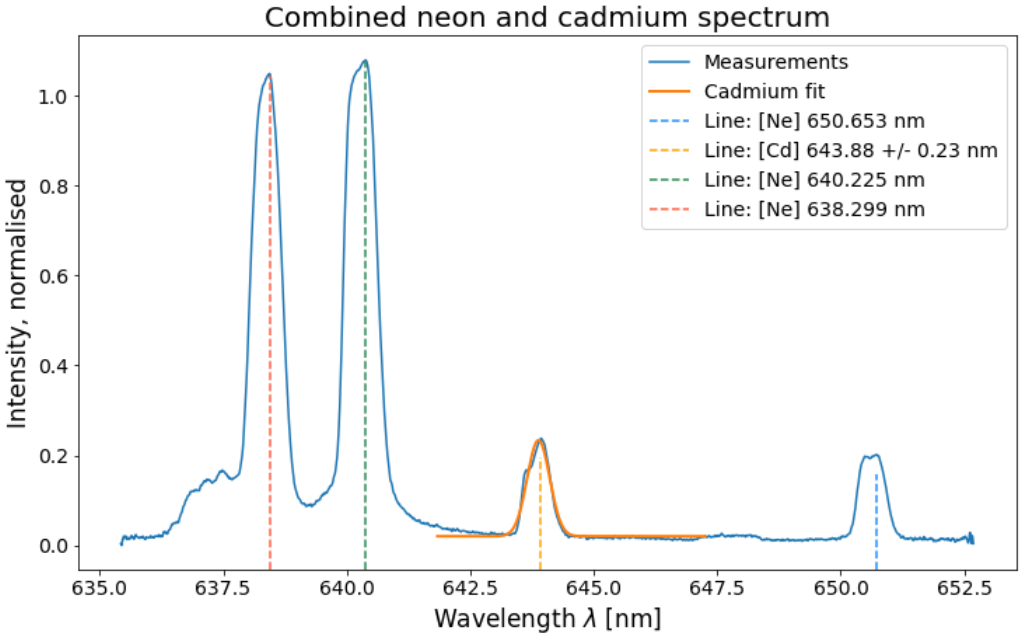


**Figure 8:** Combined spectrum of the Neon and Cadmium Lines. A gaussian curve has been fitted over the Cadmium lamp to determine the exact position and uncertainty.

# 4. Summary and discussion

## 4.1 Summary

Within the execution and evaluation of this experiment we first observed the hysteresis effect when applied to a magnetic field. For this we applied an increasing and a decreasing current.

In the next part, we measured the Zeeman spectra at 4 values for the current and fitted over each one a triple gaussian function for every corresponding order resolvable in the data. From these measurements we gathered information about the line distances within the same order and between different orders. These in turn helped us to determine the wavelength shift needed to calculate the Bohr Magneton as a conclusion to the first part.

In the second part of the experiment, which was necessary to complete the first part, we analysed the spectrum of the Cadmium lamp and determined its wavelength by comparing it to the well known specturm of the neon lamp. The wavelength we determined helped us to find the Bohr Magneton.

## 4.2 Discussion

### Hysteresis effect

First, we'll take a look at the Hysteresis effect and try to quantify its strength. One alternative is to take a look at the fit parameters of the two linear functions. For the linear part, we'd expect especially the offset parameter to be different if the hysteresis effect is strong. We will calculate the $\sigma$-deviations for a value $G \pm \Delta G$ and a comparison value $C \pm \Delta C$ as

$$\sigma = \frac{|G - C|}{\sqrt{(\Delta G)^2 + (\Delta C)^2}}. \tag{13}$$

| | Inc. | Dec. | $\sigma$ |
|---|---|---|---|
| $a$ [$\mu$T A$^{-1}$] | 0,036(1) | 0,382(5) | 1,9 |
| $b$ [$\mu$T] | 0,019(7) | 0,009(4) | 1,3 |

**Table 5:** Comparison between the fitparameters for the hysteresis effect

We can see that the effect isn't necessarily that strong. This coincides with our observations in Figure 1.

### Bohr Magneton

The next value which we can compare to literature is the Bohr Magneton. For this we used the measurements of the magnetic field (Table 1), we determined the wavelength of

the Cadmium line (Figure 8, (12)) and used the triple gaussian fits over every order to determine the relation $\delta a/\Delta a$. The magnetic field is a variable which for us is set, since it is something we measured directly while being in the laboratory. The Cadmium line appears to be according to Table 8 very near within its margins of error of the literature value. After taking the mean of the four values for the Bohr Magneton and comparing it to the literature value [1] in Table 6, we can see huge discrepancies.

| $I$ [A] | Mean | Literature | $\sigma$ |
|---|---|---|---|
| $\mu_B$ $[10^{-24}\,\mathrm{JT}^{-1}]$ | 1.9(3) | 9.27400949 | 20 |

**Table 6:** Comparison of the mean Bohr Magneton and the literature value [1]

The $\sigma$-deviation is well into the double digits. Since we've previously (next) established (will establish) that the wavelength of the Cadmium line was determined accurately, there remain the variable $\delta a/\Delta a$ and the magnetic field strength left to investigate. We can see in Figure 2 that every fit for every order is appropriate and the determination of $\delta a/\Delta a$ is also reliable. So the error can't lie in the computation of this value, except if the formulas we used to calculate it are wrong. If we assume the rest of the process to be correct within reasonable certainty, and taking a look at the likeliest suspect, the magnetic field strength, which was measured using an antiquated Hall Probe, we can conclude that it provided unreliable measurements of the magnetic field strength. We can atleast conclude for certain, that it is a systematic error plaguing our measurements, since every individual measurement for the Bohr Magneton is within good deviations from the other measurements, as seen in Table 7.

| $I$ [A] | | 8 | 9 | 11 | 12 |
|---|---|---|---|---|---|
| | $\mu_B$ $[10^{-24}\,\mathrm{JT}^{-1}]$ | 15.89(17) | 16.38(20) | 15.99(24) | 15.45(25) |
| 8 | 15.89(17) | - | 1.9 | 0.3 | 1.5 |
| 9 | 16.38(20) | | - | 1.3 | 2.9 |
| 11 | 15.99(24) | | | - | 1.5 |

**Table 7:** Comparison of the individual Bohr Magneton measurements

### Cadmium line

Interpolating the position of the Cadmium line by comparing it to the known spectrum of neon. In Table 8 we compare it to the literature value [2]

| | Measured | Literature | $\sigma$ |
|---|---|---|---|
| $\lambda_{Cd}$ [nm] | 643.88(23) | 643.847 | 0.14 |

**Table 8:** Comparison between the measured Cadmium line and the literature value [2]

### Conclusion

While the results from the Bohr Magneton measurements could indicate that the experiment was unsuccesful, which it was, it was still remarkably educational, from the theory of the Zeeman effect to the tools needed to efficiently execute the required measurements. During the experiment, it was noted that many of the things worked ineffectively, starting from the camera which was very sensible to slight movements, since there wasn't any tool with which to hold it in place for the measurements, except for duct tape, which was our preferred tool for the job. Similarly, it was noted by the tutor that the Cadmium lamp had broken and the replacement had walls which were slightly too thick to properly observe the Zeeman spectrum. For this reason, we used foreign measurements, since we couldn't properly resolve enough of the orders of interference. With little investment in proper equipment, the experiment could be more rewarding, but as it stands it can be quite frustrating to work with. Generally, however, it was a positive experience in the execution as well as the evaluation.

## References


[1] Max-Planck-Institut für Kernphysik. *Zeeman effect*. URL: https://www.physi.uni-heidelberg.de/Einrichtungen/FP/versuche/anleitungen.php.

[2] National Institute for Standards and Technology. *Strong Lines of Cadmium ( Cd )*. URL: https://physics.nist.gov/PhysRefData/Handbook/Tables/cadmiumtable2_a.htm.

# Annex

## Zeeman spectra for currents $I = \{8, 9, 11\}$ A

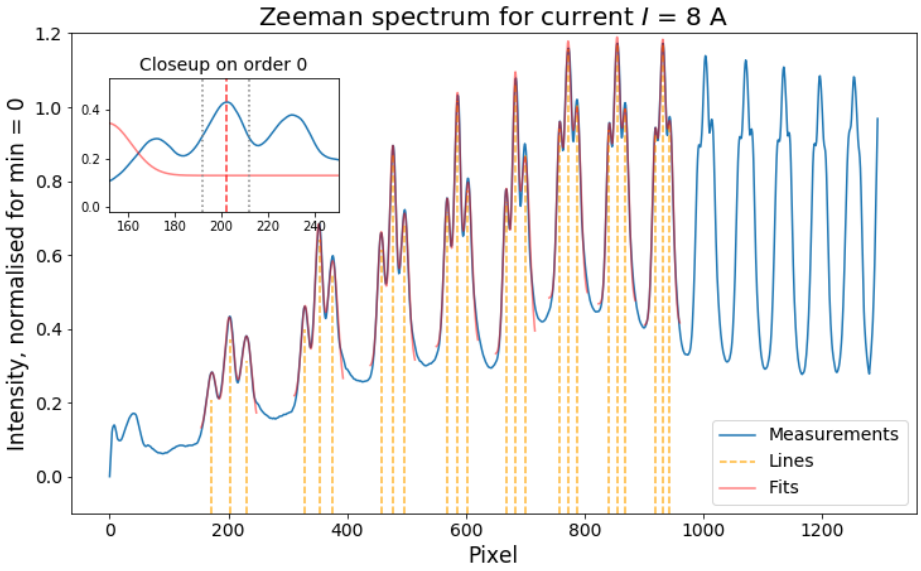


**Figure 9:** Zemman spectrum at $I = 8\,\mathrm{A}$

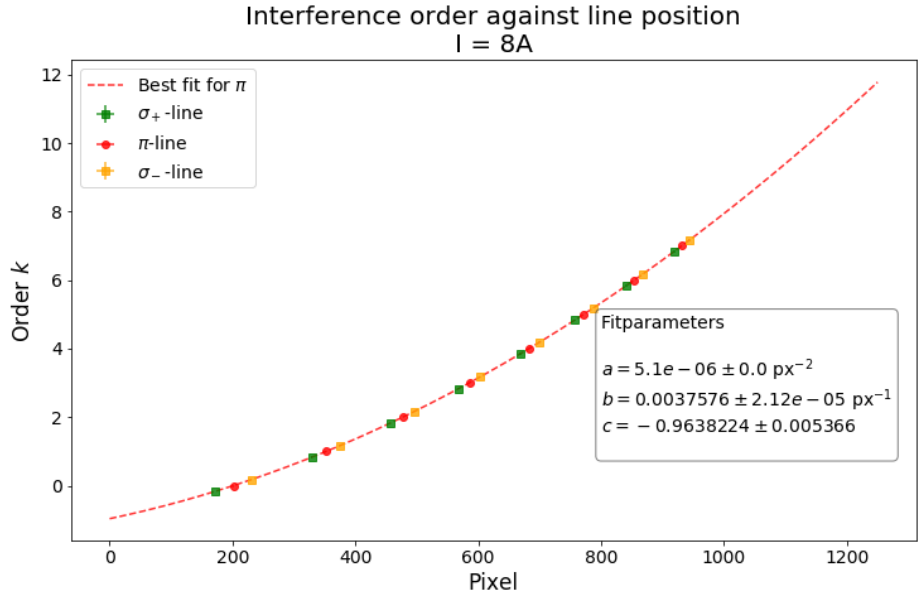


**Figure 10:** Order of interference against peak position at $I = 8\,\mathrm{A}$

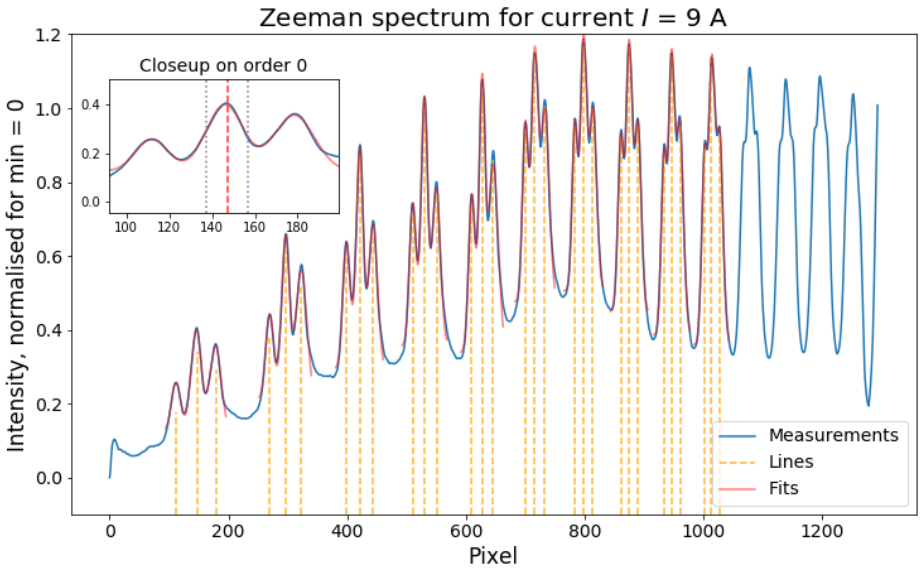


**Figure 11:** Zemman spectrum at $I = 9\,\mathrm{A}$

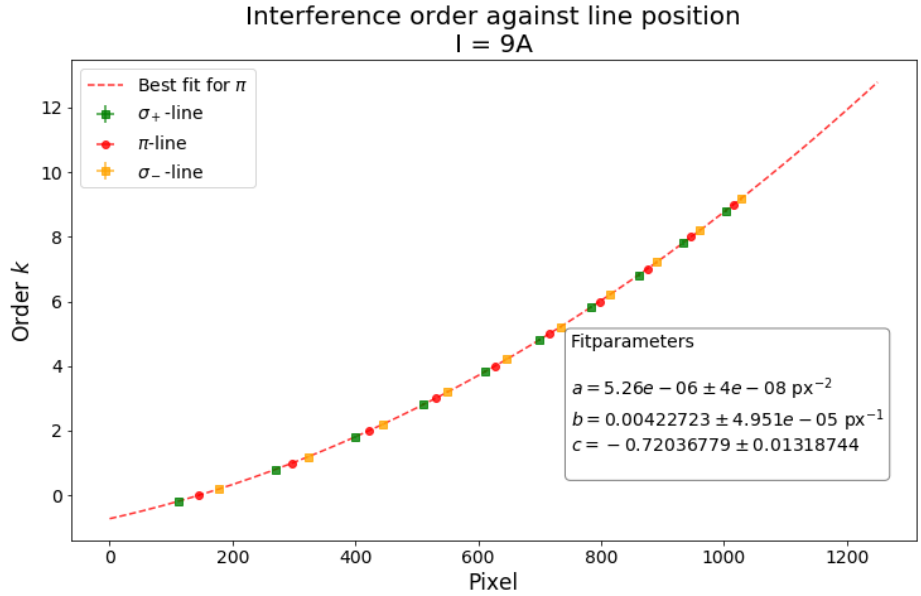


**Figure 12:** Order of interference against peak position at $I = 9\,\mathrm{A}$

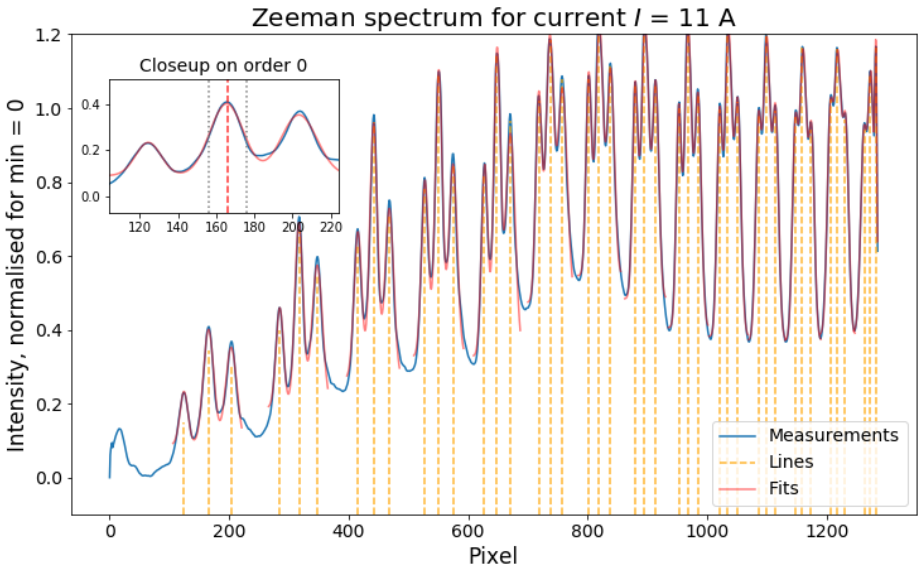


**Figure 13:** Zemman spectrum at $I = 11\,\mathrm{A}$

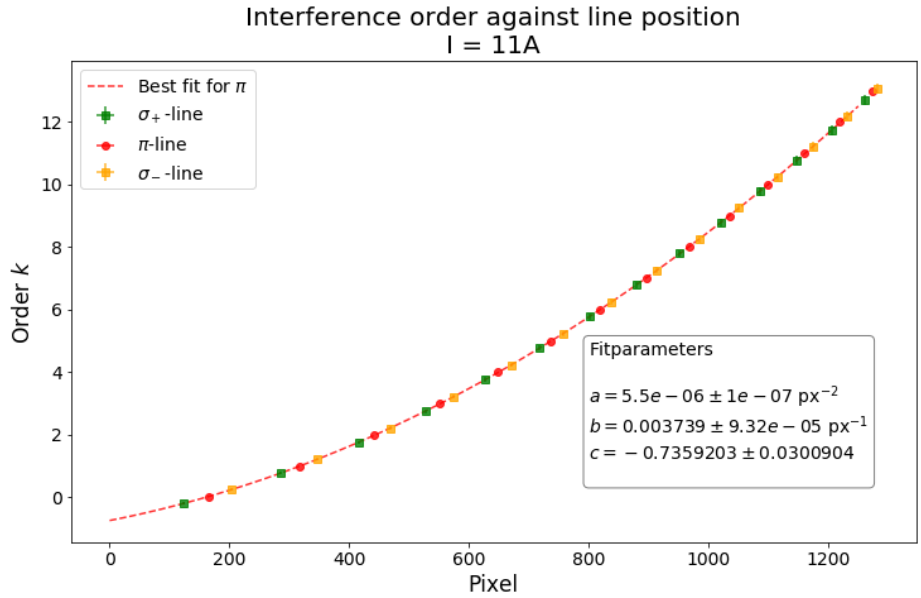


**Figure 14:** Order of interference against peak position at $I = 11\,\mathrm{A}$